Maturation of a tetravirus capsid alters the dynamic properties and creates a metastable complex

Brian Bothner[a,1], Derek Taylor[a,2], Bokkyoo Jun[b], Kelly K. Lee[a], Gary Siuzdak[a], Christian P. Schlutz[b,3], John E. Johnson[a,*]

[a]The Scripps Research Institute, Department of Molecular Biology, 10550 N. Torrey Pines Road, La Jolla, CA 92037, USA
[b]Bruker Optics, 19 Fortune Dr., Billerica, MA 01821, USA

Abstract

The assembly of monomeric protein subunits into a viral capsid is a finely tuned molecular process. In response to subtle changes in environmental conditions, this supramolecular complex can dramatically reorganize. Defining the forces that control this structure and the cooperative action of subunits has implications for biology and nanotechnology. The small icosahedral RNA tetravirus family members *Nudaurelia ω capensis* (NωV) and *Helicoverpa armigera* stunt virus (HaSV) can be purified as provirions, and maturation to capsids can be induced by a drop in pH. In this study, a comparison of capsid secondary structure using FT-IR revealed that the procapsid has more α-helical content than the capsid, supporting the proposal that helix to coil transition may be important for maturation. The dynamic properties of the two states were probed using limited proteolysis and peptide mass mapping to identify regions of significant flexibility. Interestingly, the initial sites of protease cleavage were the N and C terminal domains that are internal in high-resolution models, and to inter-subunit surfaces. Further comparison of the two particle forms using FT-IR revealed that in response to thermal stress, the provirion disassembles and unfolds in a cooperative manner over a narrow temperature range (~5 °C). Paradoxically, the capsid form, which is stable in a wide range of pH and ionic conditions and is more resistant to proteolysis, responds to thermal stress at a lower temperature than the procapsid form. This suggests that a metastable state is the end product of assembly.
© 2005 Elsevier Inc. All rights reserved.

Keywords: Tetravirus; Dynamics; Capsid; Mass spectrometry; Nudaurelia; Helicoverpa; FTIR; Metastable; Supramolecular

Introduction

Viruses must control assembly, transport, and host entry with a limited amount of genetic information. In addition, the environments for assembly and disassembly are often similar, requiring the virus to perform a thermodynamic balancing act. Small molecules that target assembly, maturation, or disassembly of virus particles are well known and demonstrate the potential for inhibiting morphogenesis with antiviral agents (Lee et al., 2004; Prevelige, 1998; Teschke et al., 1993; Zlotnick et al., 2002). In addition, the availability of structural models of the same capsid in multiple conformations makes icosahedral viruses an excellent model for studying how coordinated protein dynamics facilitate biological function.

Viral capsid protein dynamics can be divided into two general categories, large-scale rearrangements associated with particle maturation and small-scale fluctuations about a solution phase equilibrium. The large-scale protein motions

---

* Corresponding author. Fax: +1 858 784 8660.
E-mail addresses: bbothner@chemistry.montana.edu (B. Bothner), dtaylor@wadsworth.org (D. Taylor), Bokkyoo.Jun@brukeroptics.com (B. Jun), kklee@scripps.edu (K.K. Lee), siuzdak@scripps.edu (G. Siuzdak), Christian.P.Schultz@siemens.com (C.P. Schlutz), jackj@scripps.edu (J.E. Johnson).
[1] Current address: Montana State University, Department of Chemistry and Biochemistry Bozeman, MT 57917, USA.
[2] Current address: Howard Hughes Medical Institute, Wadsworth Center Empire State Plaza, Albany, NY 12201-0509, USA.
[3] Current address: Siemens Medical Solutions USA, Inc., Massachusetts General Hospital, Charlestown, MA 02129-2060, USA.

are, for the most part, irreversible and are a response to environmental signals such as nucleic acid packaging, receptor binding, or low pH (De Sena and Mandel, 1977; Fricks and Hogle, 1990; Prevelige et al., 1993). The transient and reversible small-scale dynamics have been termed breathing (Lewis et al., 1998; Li et al., 1994,). Protein dynamics in both ranges are essential to the lifecycle of a virus (for recent reviews, see Johnson, 2003; Witz and Brown, 2001).

Nudaurelia ω capensis (NωV) and *Helicoverpa armigera* stunt virus (HaSV) are members of the tetraviridea family and are positive-strand RNA viruses that infect members of the Lepidoptera order. The nonenveloped, $T = 4$ icosahedral capsids are composed of 240 copies of a 70-kDa (α) coat protein that, after assembly, autocatalytically cleaves creating 62-kDa (β) and 8-kDa (γ) proteins (Agrawal and Johnson, 1995; Munshi et al., 1996). In the capsid form, the subunits adopt four slightly different conformations (A, B, C, and D) consistent with the theory of quasiequivalence (Casper and Klug, 1962). A cell culture system for these viruses has not been established; therefore, a recombinant baculovirus system was used to express capsid protein that spontaneously assembles into virus-like particles (VLPs). These particles package heterologous cellular RNA at a similar ratio to protein as authentic virions (Canady et al., 2000). Analysis of VLPs purified at pH 5.0 by cryoEM and image reconstruction showed that they are morphologically indistinguishable from authentic virions with an average diameter of 395 Å (Canady et al., 2001). Purification of VLPs above neutral pH preserves the procapsid form which is 485 Å, nearly spherical, fenestrated at the symmetry axes, and has sparse interfacial contacts.

The transition from procapsid to capsid can be induced by lowering the pH from 7 to 5 (Fig. 1). Structural
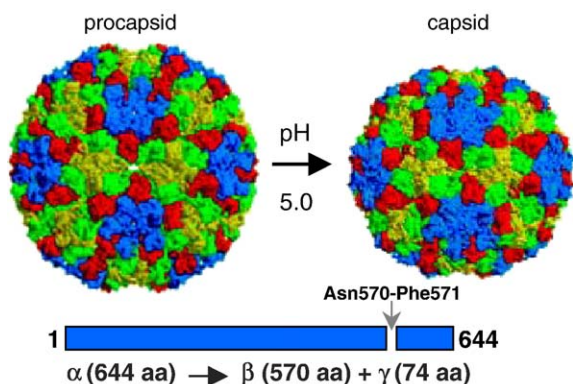

Fig. 1. pH-induced maturation of the T4 icosahedral omega-tetraviruses. The rearrangement of subunits in the transition from procapsid to capsid involves mostly rigid body translation and rotation with limited refolding of the internal helical domain. 240 copies of β and γ are present in each mature particle in 4 quasi-equivalent positions (A = red, B = blue, C = green, D = yellow).

rearrangement occurs in less than 100 ms at pH 5.0 and occurs in a highly cooperative manner between pH 6.7 and 6.0 (Canday et al., 2000). Formation of the capsid form activates the autoproteolytic cleavage between residues 570 and 571 converting α (1–644) into β (1–570) and γ (571–644) (Canady et al., 2001). Cleavage occurs on a timescale of hours and re-expansion of the particle is possible until ~15% of the subunits have cleaved. Fitting of the X-ray coordinates from capsid into the cryoEM image reconstruction demonstrates that conversion depends largely on quaternary reorganization with only limited refolding (Canday et al., 2000). The refolding that does occur is located in the helical domain that forms the inner surface of the capsid and is in contact with the RNA. Currently, there are two models that describe the driving force for this dramatic rearrangement. A helix to coil unfolding in the γ-peptide was proposed by Taylor et al. (2002). More recently, the unusual arrangement of carboxylate side-chains at the subunit interface was sited as a candidate for controlling the pH-dependent transition (Helgstrand et al., 2004).

Superimposed on the large-scale protein rearrangements are fluctuating protein dynamics. These fluctuations can involve externalization of domains clearly shown to be internal in the structural models. The first evidence for capsid breathing came from antibody binding experiments with poliovirus (Li et al., 1994). A more quantitative approach using limited proteolysis and peptide mass mapping improved the resolution and allowed comparisons of the dynamic regions to be made (Bothner et al., 1998, 1999; Lewis et al., 1998). Fluorescence and NMR experiments have also contributed to the solution phase behavior of viral particles (Oliveira et al., 2000; Vriend et al., 1986). Chemical reactivity of particles is also influenced by dynamics, presumably by altering the solvent accessibility of residues (Bothner et al., 1999; Taylor et al., 2003). In solution, icosahedral virus particles are now understood to exhibit a dynamic character that is not readily inferred from the high-resolution structure models.

Here we seek to understand the biophysical and biological role that protein dynamics play in icosahedral viral particles. The pH-induced transition from procapsid to capsid of these $T = 4$ icosahedral viruses provides a direct comparison of the dynamics of an assembly intermediate with the final product. To this end, we have applied site-directed chemical labeling and limited proteolysis in conjunction with mass mapping to localize dynamic regions of the capsid protein. The first application of FT-IR spectroscopy to the study of capsid protein structure provides spectroscopic evidence for a helix to coil transition during maturation of NωV. The mature capsid form is less dynamic than procapsid, as determined by protease digestion and chemical labeling. There is also a difference in the chemical reactivity and protease accessibility of γ-peptides in $T = 3$ and $T = 4$ insect viruses, suggesting that they may have different functions. Interest-

ingly, protein regions that are internal in the structural models are initially the most susceptible to proteases. Thermal stress experiments comparing procapsid and capsid reveal that while procapsid behaves in a highly cooperative manner to thermal stress, capsid has a biphasic response. In contrast to the chemical reactivity and proteolytic experiments, the capsid form reacts at a lower temperature than procapsid when heated, suggesting that maturation leads to a metastable state. The receptor and possibly other factors then act as a transition-state catalyst to overcome the energy barrier to RNA release and uncoating.

Results

Maturation of VLPs changes secondary structure content

Fourier transform infrared spectroscopy is a powerful technique for studying the secondary structure of proteins. Absorption in the IR range by the peptide amide bond is dependent on the hydrogen bonding pattern, and therefore the local secondary structure of the backbone. NωV capsid and procapsid samples in 50 mM Tris–HCl, 250 mM NaCl (pH 7.6) were used for the analysis. After extensive dialysis against buffer made with D_2O, the samples were concentrated to 7 mg/ml. The attenuated total reflectance infrared spectra (ATR-IR) of procapsid and capsid showed that the two forms of VLPs significantly differed in the amide I region (Fig. 2). Secondary structural elements have specific absorption bands in this region from 1600 and 1700 cm^{-1}; α-helical structures have bands between 1649 and 1657 cm^{-1}, most β-strand-containing structures have bands between 1620 and 1638 cm^{-1} and in case of anti-parallel β-strands a second band usually between 1675 and 1678 cm^{-1} (Schultz, 2000). A comparison of the two spectra revealed that there was significantly larger contribution from helix in the procapsid form, while the capsid form contains more anti-parallel β-strand structure. This means that on conversion to capsid, the relative contribution from β-strand increased. Substantial regions of capsid protein were not visible in the atomic model of NωV. The missing regions correspond to the N- and C-termini and are localized to the interior of the capsid (Munshi et al., 1996). Electron microscopy studies are consistent with this observation because a significant rearrangement of the internal domains of NωV was required when the subunit model from capsid was fit into the cryoEM model of the procapsid (Canday et al., 2000).

Stability of tetraviruses to protease

Maturation results in a particle that can protect the packaged RNA and deliver it to the next host cell. The capsid form is more stable to changes in pH and ionic
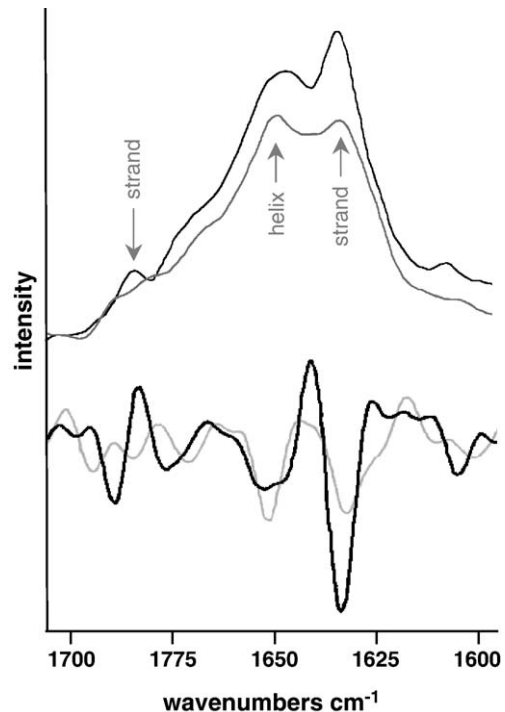

Fig. 2. FT-IR analysis of procapsid and capsid secondary structure. Upper curves are the direct signal from the ATR biocell after buffer subtraction, lower curves represent the second derivative. The amide 1′ region of the FT-IR spectrum for NωV procapsid (gray) has a strong α-helical contribution (~1650 cm^{-1}). After maturation, the capsid (black) has a weaker relative α-helical contribution and more prominent β-strand bands (1634 and 1685 cm^{-1}).

strength, and it was therefore of interest whether this stability was specific to chemical stress or was of a more general nature. To test this, the stability of procapsid and capsid forms of NωV and HaSV was investigated by digesting the samples with protease. VLPs before and after maturation were incubated with trypsin (1000:1, wt/wt) in buffer A. Protease reactivity was monitored by SDS–PAGE analysis. A time course of the proteolysis (Fig. 3A) revealed that the capsid form of the particles is more resistant to digestion. After 24 h of digestion at room temperature, both the β protein and the γ-peptide are still present in the capsid sample whereas the α-protein band from procapsid was mostly digested by 3 h.

Because it is not feasible to identify individual peptides with gel electrophoresis, we analyzed the samples using MALDI-TOF. Initially, capsid and procapsid of NωV and HaSV were digested for 1 h with trypsin. The samples were then diluted 10-fold into 50 mM Acetic Acid to inhibit further digestion and insulin β-chain peptide was added as an internal ionization standard. Ion intensity of all tryptic peptides below 5000 Da was summed and divided by the intensity of the internal standard. The relative peptide ion intensity was approximately 5 times greater from procapsid when compared with the capsid samples for both tetravirus
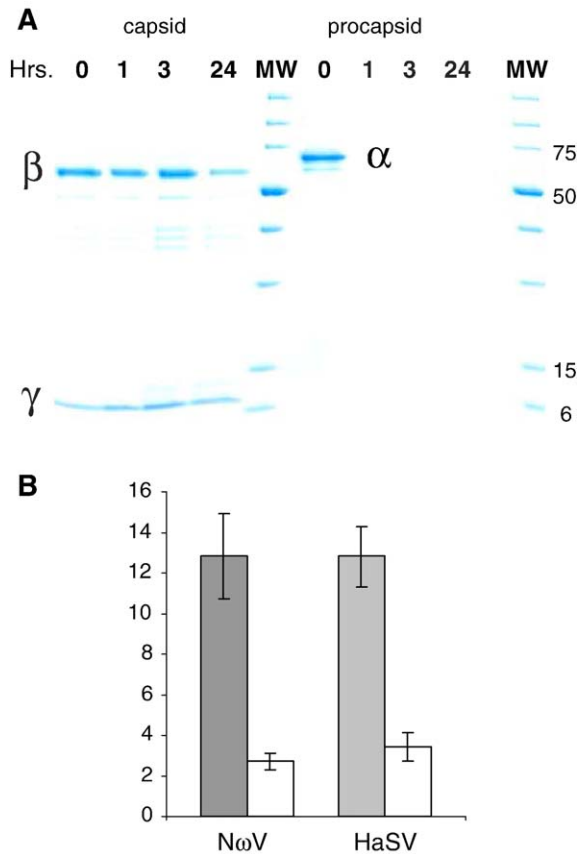
Fig. 3. Comparison of tetravirus procapsid and capsid resistance to protease digestion. (A) SDS–PAGE analysis of a time-course incubation of NωV capsid and procapsid with trypsin (1000:1 w/w). The β and γ forms of capsid protein are visible on the left and the intact a precursor protein is right of the marker. (B) Relative ion intensity of released peptides compared to an internal standard using MALDI-TOF mass spectrometry (n = 3). Procapsid in gray and capsid in white.

family members (Fig. 3B). These data represent three separate experiments in which each sample was analyzed by MALDI-TOF three times.

Protease mass mapping

The exact location of cleavage sites that lead to the release of the peptides analyzed in Fig. 3 is of interest. To this end, we sampled the digestion of VLPs at 5, 10, 20, 60, and 180 min. MALDI-TOF analysis was carried out as described above without the addition of an internal standard. The molecular weights of the released peptides were then searched against the amino acid sequence of NωV or HaSV and mapped onto the capsid protein. At the early time points, the majority of peptides were from the N and C termini in both procapsid and capsid samples (Fig. 4). Residues identified at trypsin cleavage sites after a 5-min incubation were: R15, K27, R32, R39, R75, R79, K94, R106, R216, R233, K447, K458, R484, R495, K514, K588, K597, R613, K628, R633 in NωV and R15, R22, R32, R33, R36, K81, K97, R109, R217, R236, K463, R489, R491, R500, R515, K593, K602, K629, R635, R637, R641 in HaSV. Peptides spanning residues 1–109, 484–514, and γ-peptide were well represented. The protein regions mapped in NωV and HaSV are very similar even though only 50% of the cleavages occur at conserved residues. The overall pattern of procapsid and capsid maps is similar, although the intensity of peptides was much greater in the procapsid samples as described above (Fig. 3B).

When the initial tryptic cleavage sites were mapped onto the quaternary model of the NωV subunit, most were located below the particle surface (Fig. 5). Models of the NωV capsid and procapsid from X-ray and cryoEM data, respectively, show these domains to be internal, with close proximity to the packaged RNA (Canady et al., 2000). Residues 90–110 are at the subunit interface and contain acidic residues implicated in the pH-driven transformation (Helgstrand et al., 2004). Residues 480–510 form the top of the β-barrel fold, beneath the Ig domain, and represent the most surface exposed of the early cleavage regions. Peptides from each
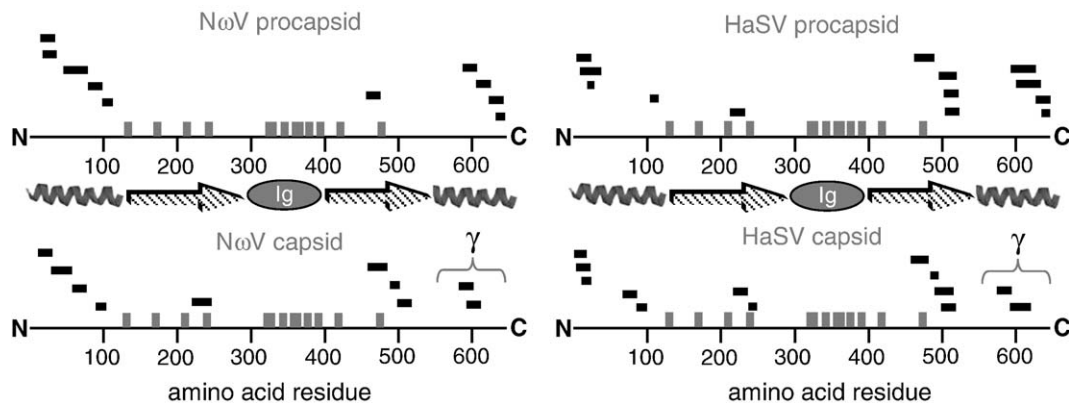

Fig. 4. Initial trypsin cleavage sites on tetravirus particles. Procapsid and capsid forms of NωV and HaSV were digested with trypsin to reveal the dynamic regions of protein. Peptides were identified using MALDI-TOF after a 5-min incubation with trypsin (1000:1 w/w). x-axis is amino acid residue number from the N to the C terminus. The domain structure of the capsid protein is represented with coils for the internal helical regions and arrows for the β-barrel. Horizontal black bars span residues present in protease released peptides and the vertical gray bars indicate residues on the surface of the particle.
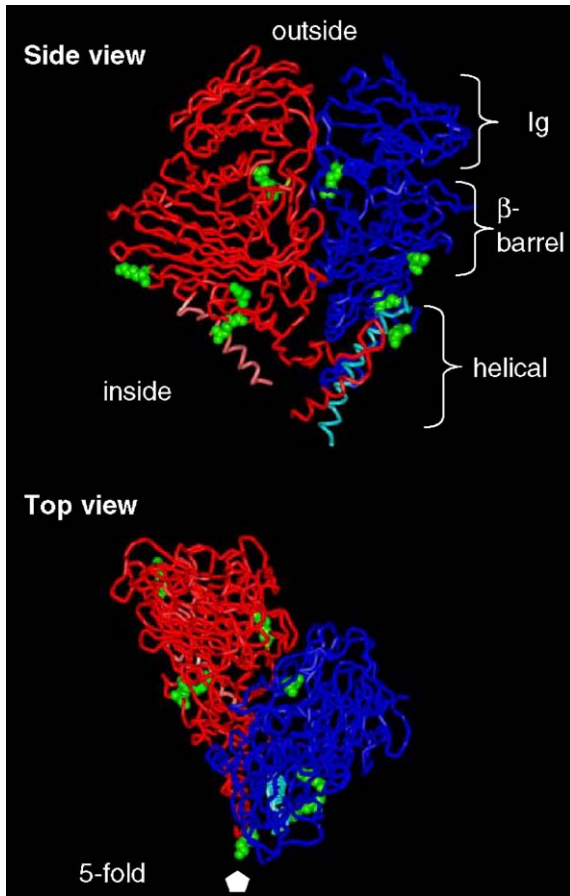
Fig. 5. Subunit model of NωV mapped with first sites accessible to protease. Two of the four quasi-equivalent folds in the T4 architecture are depicted, A fold in red and B fold in blue. γ-peptides are in pink and cyan. Representative cleavage sites are depicted with green sidechains. For clarity, selected sidechains are displayed where residues are very close in 3D space. Residues 1–40 and 598–646 occur in regions not visible in the model. The helical domain is formed by the N- and C-terminal regions and interacts with packaged RNA.

of these four regions were also identified when the experiments were carried out with the protease Glu-C, which cleaves at glutamic and aspartic acids.
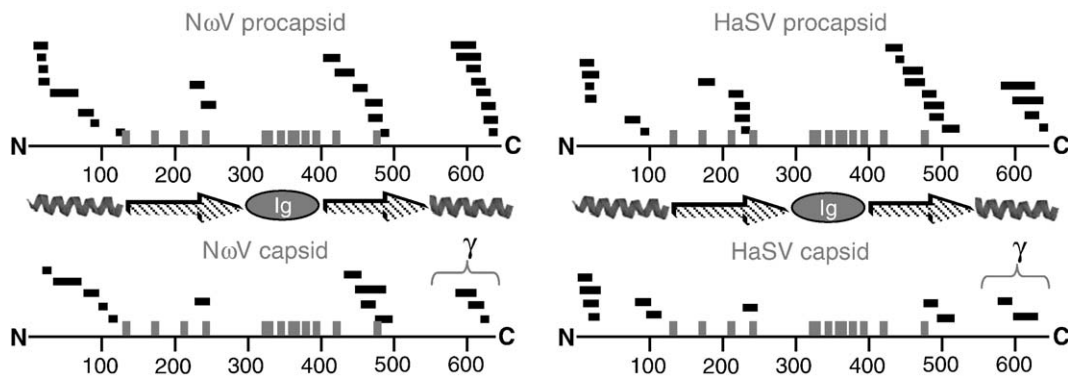
As the proteolysis reaction continued, a steady increase in overlapping peptides from both termini, top of the β-barrel below the Ig domain (447–514), and a fourth region (217–233) which contains a short strand and helix that have been inserted into the canonical β-barrel between strands C and D were identified (Fig. 6). Residues in the NωV β-barrel domain that were cleaved were on the edge of the jelly-roll fold. Residues R233 and R485 are on top of the β-barrel, underneath the Ig domain. Prolonged digestion of the VLPs led to the generation of an overlapped map of peptides that covered the entire protein except for the Ig domain. In our analysis of the mass mapping experiments, we focused only on the early time points (<20 min) because as cleavages accumulated the particles would be destabilized.

Chemical reactivity of γ-peptide

The icosahedral capsids of T = 3 nodaviruses and T = 4 tetraviruses share an autoproteolytic event in their maturation that generates a peptide which remains associated with the particle. The mechanism, location, and quaternary structure all suggest that these are homologous structures. Previously, we demonstrated that the γ-peptide of FHV, a member of the nodavirus family, readily reacts with small molecules specific for primary amines (Bothner et al., 1999). Experiments with HaSV and NωV showed that butanoic anhydride, biotin succinimidyl ester, and acetic anhydride react with the γ-peptides. Therefore, we were interested to compare the reactivity of the T = 3 FHV γ-peptide with the T = 4 tetravirus version of the peptide. FHV and HaSV particles (20 μM protein) were incubated with 1% butanoic anhydride for 1 h at room temperature. Samples were then analyzed by MALDI-TOF to look for covalent modification of lysine sidechains and the N-terminus of γ-peptide. FHV γ-peptide reacted with the addition of up to 3 molecules of butanoic acid (Fig. 7). In contrast, the γ-peptides from HaSV and NωV were not labeled after 1 h, indicating slower reaction kinetics.

Fig. 6. Peptide maps after incubation of NωV and HaSV with trypsin for 20 min. Dynamic regions of the capsid proteins are represented with overlapping peptides.
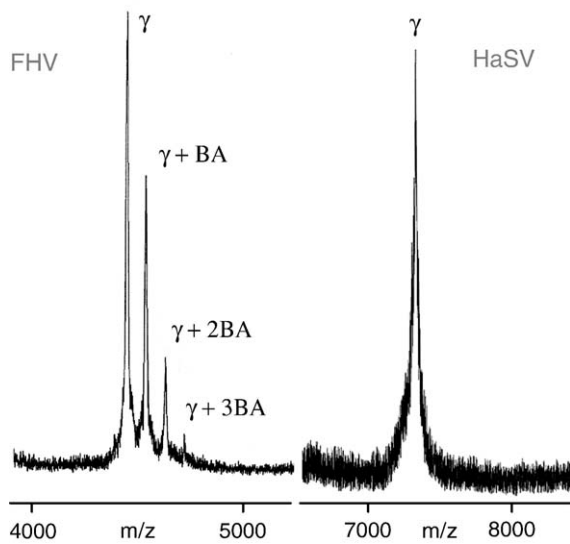
Fig. 7. Chemical reactivity of γ-peptide in T3 and T4 icosahedral capsids. The amine reactive compound butanoic anhydride readily reacts with the T3 FHV γ-peptide whereas the T4 HaSV has not reacted after 1 h. NωV γ-peptide is also unreactive in the first hour under the same conditions, but both tetravirus γ-peptides can be fully labeled if the reaction is allowed to proceed.

Effect of ionic strength on capsid dynamics

Tetravirus VLPs in the procapsid form are unstable in low (<0.1) or high (>0.5) ionic strength solutions. For this reason, all of the previous experiments were carried out in the presence of 250 mM NaCl. The mature capsid form of the VLPs is stable for extended periods in low or high salt. To test the effect of ionic strength on dynamics, NωV and HaSV particles were rapidly exchanged into 25 mM Tris–HCl (pH7.6) and trypsin digestion was repeated. In low salt buffer, disrupted procapsids are visible by negative stain EM after 24 h. Proteolysis under these conditions was more rapid and more strongly localized to the N and

C terminal domains of the capsid protein (Fig. 8). Lowering of the ionic strength altered the capsid behavior, changing the kinetics of cleavage such that the termini were more specifically targeted. The similar effect on both capsid and procapsid of ionic strength raised the question, would both forms respond to temperature in the same way?

Response of procapsid and capsid to thermal stress

The protein subunits in a procapsid behave in a highly cooperative manner when the pH is lowered, rapidly reorganizing to the mature capsid state (Canady et al., 2000). We were interested to know whether other physical or chemical changes would also induce cooperative behavior and if the mature form in which the subunits have adopted their quasi-equivalent positions behaved similarly. FT-IR analysis is readily amenable to thermal denaturation studies. The ATR cell utilized for measuring microvolume samples (~10 microliters) is tightly sealed, so no precautions for evaporation need to be implemented. NωV samples were heated in 5 °C steps from 20 to 90 °C. The reaction to thermal stress was fundamentally different for procapsid and capsid (Fig. 9). A plot of the intensity of the native secondary structure versus temperature showed that the procapsid had a cooperative loss in structure at ~69 °C, over a narrow temperature range (<10 °C) (Fig. 10A). In contrast, the capsid had a more complicated response. The first significant change in the capsid occurred at ~50 °C, followed by a slight unfolding, and then a second decrease (~80 °C) in native structure. FT-IR is sensitive to changes in hydrogen bonding between β-strands. We followed the intensity of the signal at 1617.5 and 1684 cm^{-1}, which correspond to hydrogen bonds in anti-parallel β-strands formed during partial restructuring and protein aggregation (Krimm and Bandekar, 1986). Once again, the procapsid had a single transition over a narrow temperature range, whereas the capsid exhibited biphasic behavior (Figs. 10B and C). The strong signal for β-strand at high temperatures
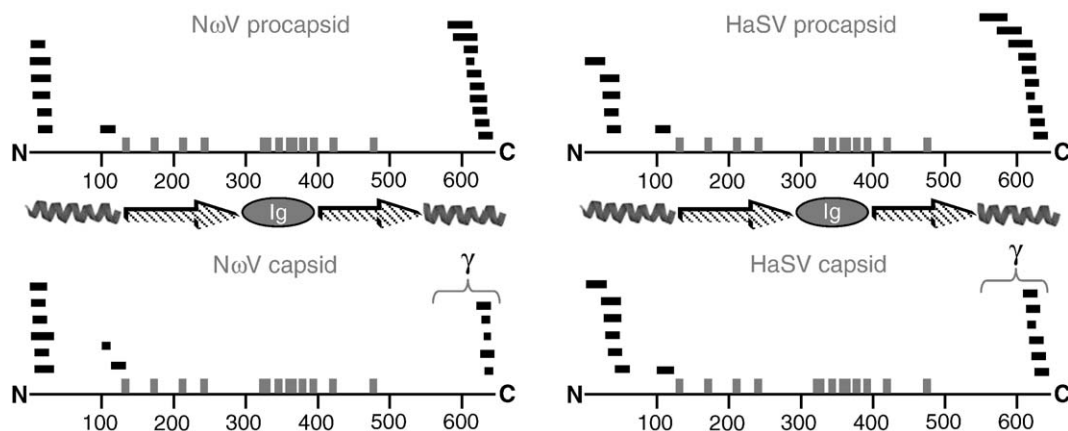

Fig. 8. Limited proteolysis at low ionic strength. Ionic strength alters the cleavage pattern and rate of digestion for NωV and HaSV procapsids and capsids.
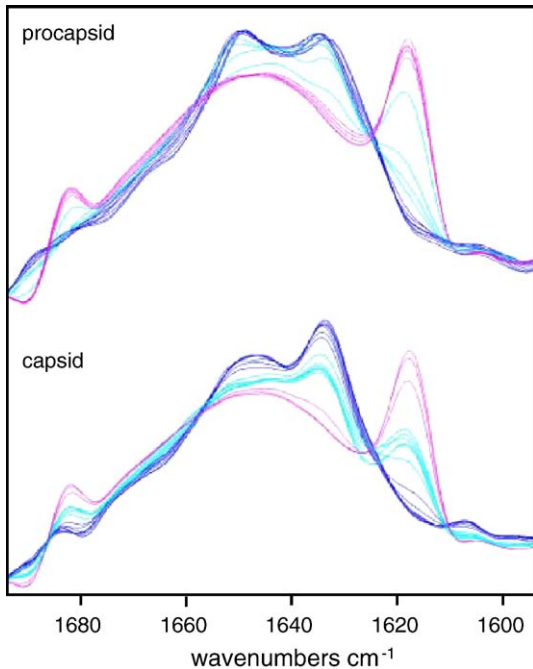
Fig. 9. FT-IR analysis of NωV thermal denaturation. NωV procapsid (upper) and capsid (lower) heated from 20 to 90 °C. Blue to red traces follow the heating in 5 °C steps. Procapsid exhibits a cooperative response, unfolding, and then aggregating. Capsid secondary structure changes in two steps, unfolding and aggregating simultaneously.

is characteristic of irreversible aggregation (Casal et al., 1988; Zurdo et al., 2001).

Discussion

Structural models of icosahedral virus capsids are important for understanding the biophysical properties that govern assembly, packaging of nucleic acid, and infection. Studies of the same particles in solution have demonstrated that the static models from X-ray and cryoEM only tell part of the story. Biochemical and biophysical experiments reveal that, in fact, capsids are highly dynamic complexes whose functionality requires protein dynamics on multiple scales. Often, the protein domains of greatest biological interest are not visible in the structural models. In this study, we used solution-based techniques in an attempt to elucidate the role of protein dynamics in two small RNA viruses.

The structural reorganization of NωV and HaSV, that leads to autoproteolysis, involves large-scale movements that decrease the particle diameter by >15% and local refolding of internal helical regions of the capsid protein. Previous evidence for refolding came from fitting the subunit coordinates from the NωV capsid into the cryoEM map of the procapsid. Density at the 3-fold and quasi 3-fold axes is lost during the transition to capsid, implying that α-helical regions in the A and B subunits either become disordered or no longer conform to icosahedral symmetry

(Canday et al., 2000). Our FT-IR analysis of the two particle forms clearly shows that the secondary structure composition is different (Fig. 2). Bands from the α-helical region diminish while there is a relative increase in β-strand upon conversion to capsid. The overall increase in signal is a reflection of the numerous inter-subunit contacts present in the capsid, compared with the relatively sparse contacts in the procapsid.

Currently, there are two models for the pH-driven maturation process. A helix to coil transition of γ-peptides in the A and B quasi-equivalent subunits was proposed by Taylor et al. (2002) and is consistent with the loss of density in the helical domain upon maturation. In this model, autoproteolytic cleavage would disconnect the driving force for conformational change from the rest of the capsid, explaining why the process is not reversible once cleavage has occurred. A more recent model based on the refined X-
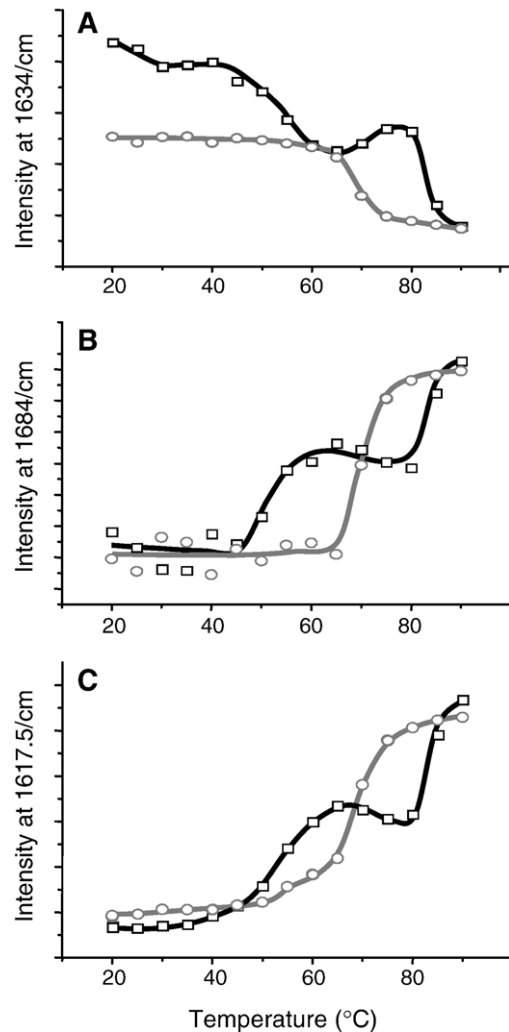

Fig. 10. Thermal response of selected NωV features. Change in individual bands from the FT-IR amide I region as samples were heated from 20 to 90 °C in 5 °C steps. Procapsid circles (gray) and capsid squares (black). Native structure (A) and β-strand regions (B and C). Smooth curves are a guide to ease viewing.

ray structure of the capsid at pH 6.5 suggests that clusters of acid residues at the subunit interface cause expansion above the pI of the acidic residues due to charge repulsion (Helgstrand et al., 2004). While the data presented here confirm that refolding occurs upon maturation, the driving force for this rearrangement remains unresolved. Mutagenesis of residues in the acidic cluster could help to elucidate this point.

Limited proteolysis of the VLPs shows that procapsid digests at least 5 times faster than capsid based on MALDI-TOF analysis of the released peptides and SDS–PAGE analysis of intact protein. The decreased accessibility and/or flexibility of the capsid that we have detected mirror the stability of mature NωV and HaSV VLPs to a wide range of ionic strength and pH conditions. The total numbers of inter-subunit contacts calculated from subunit coordinates modeled into the cryoEM map for procapsid and the X-ray coordinates for capsid are 17,520 and 107,520, respectively (see VIPER website; Reddy et al., 2001). This large increase in intermolecular contacts between subunits stabilizes the particle, but as we have demonstrated, does not quench all of the solution phase dynamics.

Protease mass mapping provides information on the flexibility and accessibility of the peptide backbone in proteins and protein complexes (Bothner et al., 1998; Cohen et al., 1995; Fontana et al., 1986; Kriwacki et al., 1996). The mapping data presented here reveal that the kinetically favored sites are inside the capsid based on the structure models. Initial sites localize to the N and C termini (which are internal), subunit interfaces (buried), and below the Ig domain (buried). The prominent Ig domain, which sits atop the subunit and is the most highly solvent exposed region, remains uncleaved even after 3 h of digestion. Ig domains are often present in cell surface and secreted proteins and are known to be tightly folded globular domains (Brandon and Tooze, 1998).

The kinetics of proteolysis at any given site is highly dependent on the structural context. It is possible that the proteases could be selecting for a specific secondary element rather than polypeptide chain flexibility. To see if secondary structure influences accessibility, we compared the cleavage sites in both capsid and procapsid after a 5-min trypsin incubation with all potential sites. Twenty Arginine and Lysine residues were protease sensitive, 11 of which are in loops or not visible in the X-ray structure. Nine of the sensitive sites are therefore in helices or strands. For the Arginine and Lysines which are not targeted, 19 are in loops or not visible while 16 are in helices or strands. Comparing the accessible to the inaccessible residues gives 45% and 46% in defined secondary elements, respectively (Table 1). This demonstrates that the site-specific kinetics of proteolysis are based on criteria other than the local fold. The fact that nearly half of the cleavage sites are within defined secondary elements is a strong reminder that the solution phase behavior of a protein is not always obvious from the structural model.

Table 1
Secondary structure and trypsin selectivity in NωV particles (5-min digestion)

Secondary structure	Helical/Strand	Loop/Disordered	Percentages
Cleaved	9	11	45/55
Uncleaved	16	19	46/54

The resolution of limited proteolysis is related to the sequence specificity of the proteases and the protein sequence. The parallel analysis of NωV and HaSV removes some of the sequence-induced bias inherent in this technique. Overall sequence conservation between NωV and HaSV is ~70%, with 40 out of 61 basic residues conserved. Structurally, these two subspecies are very similar (D. Taylor and J. Johnson, unpublished data). The helical region, the inner most domain of the capsid protein, has 64% identity between NωV and HaSV and sustained the majority of the early cleavages. After the 5-min incubation with trypsin, 36% (20) of all the possible cleavages in NωV were identified. Of these accessible sites, 50% (10) are conserved in HaSV. Viewed in another way, 50% of the cleavage sites are at different positions, yet the overall peptide maps are closely similar (Fig. 4).

Transient exposure of internal domains to the capsid surface has been well documented in the picornavirus family (Lewis et al., 1998; Li et al., 1994) and for Flock House virus (Bothner et al., 1998), another small RNA virus. The data presented here demonstrate that $T = 4$ icosahedral capsids also transiently expose internal domains and inter-subunit contact surfaces in solution. The solution phase, capsid protein dynamics, identified in this study of tetraviruses is believed to be an integral component of viral capsid function. The use of drug-resistance mutants to identify functional regions in picornavirus capsid proteins indicates that similar dynamics are required for infection (Li et al., 1994; Mosser et al., 1994; Reisdorph et al., 2003).

A surprise in the mapping data was the similarity of the patterns between procapsid and capsid. The dramatic reorganization and presence of 6 times as many inter-subunit contacts have only a moderate effect on the pattern of cleavage. Apart from the increased stability upon maturation, the biggest change is a relative decrease in sites mapping to the γ−peptide. Analysis by SDS–PAGE shows that γ-peptide is still present after 24 h. Our previous work with FHV virus demonstrated that the γ-peptide was highly accessible to protease digestion and site-directed labeling (Bothner et al., 1998, 1999). This is a fundamental difference between noda and tetraviruses, as the C-terminus in NωV and HaSV becomes less accessible once it has cleaved to become the γ-peptide.

The recent publication of the refined structure of NωV (Helgstrand et al., 2004) provides a structural basis for this finding. In FHV, a helical bundle of 5 amphipathic helices is positioned below the capsid surface at the 5-fold axis of symmetry and has been implicated in the penetration of membranes and RNA release (Bothner et al., 1998; Cheng et

al., 1994; Janshoff et al., 1999). A similar structure was originally reported in NωV, but now that the X-ray data have been fully refined, an extra helix from the N-terminus of the neighboring B subunit is positioned between the γ−peptide helices, creating a 10 helix structure. Significant rearrangement would have to occur in order for γ-peptide to reach the surface.

A limitation of the mapping techniques employed here is that quasi-equivalent conformers cannot be discriminated. For example, the capsid forms of NωV and HaSV are both stable at low ionic strength; however, this altered the accessibility of the capsid protein termini to protease. Whether this is due to a general increase in capsid dynamics or a specific effect on one region of the capsid is not known. The ability to follow the kinetics of proteolysis more precisely could potentially reveal the influence of quasi-equivalence. While the physiological relevance of the behavior of VLPs at low ionic strength is currently not understood, clearly this demonstrates that there are conditions in which γ-peptide is readily exposed to the capsid surface.

The role of the viral capsid protein is to package, protect, and deliver genetic information to a host cell. To this end, assembly of icosahedral viral capsids is often a multi-step process that generates a particle poised for attachment to a host cell and subsequent release of nucleic acid. Essentially, assembly is an energetically favorable process that creates a stable supramolecular complex. Receptor binding and/or cell entry provide the energy to breach the thermodynamic barrier to disassembly.

The structural transition from procapsid to capsid changes the stability and fundamental behavior of the particles. In response to low pH, $T = 4$ procapsid rearranges in a highly cooperative manner (Canady et al., 2000). Thermal stress has a similar effect on the procapsid. Spectroscopic analysis of multiple structural elements during heating shows that there is a large change in structure that occurs over a narrow temperature range (Figs. 9 and 10). The loss of native secondary structure and appearance of aggregated β-strands occur in a single transition, typical of an assembly of identical parts. Mature particles react differently to thermal stress. First, there is a biphasic nature to each of the heating curves. Second, the low temperature step occurs below the cooperative transition of procapsid. Whereas procapsid is stable to above 70 °C, capsid begins to change near 50 °C. This change is limited and most of the native structure is retained. If heating is continued, a second more dramatic change occurs above 80 °C where the virus irreversibly aggregates.

The procapsid form of a virus often has sparse interfacial contacts (Canady et al., 2000; Conway et al., 2001; Liu et al., 2003) and maybe sensitive to pH and ionic conditions. Remarkably, we have identified conditions under which the mature form is more sensitive and believe that this is relevant to the biology of the virus. The life cycle of a tetravirus exposes it to pH and ionic strength variations as it

is released from apoptotic midgut cells, is passed from the insect, and awaits ingestion by the next host. On the other hand, virus particles would not normally encounter temperatures above 50 °C. In light of this finding, it is interesting to speculate that temperature is mimicking an event normally caused by receptor binding. Negative stain EM analysis of NωV capsid heated to 55 °C for 10 min reveals no obvious change in the capsid surface. This suggests that the initial structural change induced by temperature maybe reversible or affects only internal domains. Heating above the transition temperature for procapsid and the high temperature transition for capsid leads to visible aggregation and is not reversible. At this point, it is not known if temperature is inducing a breathing mode in the mature tetravirus, as occurs with picornaviruses at body temperature (Joklik and Darnell, 1961), or if this transition is more akin to the generation of the picornavirus A particle which maybe an infection intermediate (Fenwick and Cooper, 1962). The concept that maturation leads to the formation of a metastable complex has been explored with poliovirus (Hogle, 2002). Computational studies have also been helpful in understanding the basis of human rhinovirus particle stabilization by small hydrophobic compounds (Phelps and Post, 1995). Analogous to the studies with human rhinovirus and drug binding, the tetravirus maturation process may stabilize the particles by increasing the entropy of the complex.

The fact that structural models are available for both the procapsid and capsid form of NωV and the similarity of HaSV make this an excellent system for studying small- and large-scale protein dynamics. Understanding the coordination of protein motion within these small RNA virus capsids will undoubtedly be applicable to not only to other viruses, but also to supramolecular complexes in general.

Materials and methods

Isolation of VLPs

NωV and HaSV capsid protein were expressed using recombinant *Autographa californica* mononuclear polyhedrosis virus as previously described (Canady JMB 2000). Individual plaque isolates were amplified and infectivity titers were determined using standard protocols. Briefly, T. ni insect cells at 2×10^6/mL were infected with recombinant baculovirus (pBacPAK6) at 5 PFU/cell and cultured for 5 days after which cells were lysed with 0.5% (vol/vol) NP-40 detergent. The supernatant, which contained the virus, was separated from debris by centrifugation at $10,000 \times g$ for 20 min. VLPs were then pelleted through a 30% (wt/vol) sucrose cushion at pH 5.0 (capsid form) or pH 7.6 (procapsid form). VLPs were purified as procapsid in 50 mM Tris–HCl, pH 7.6, 250 mM NaCl, 5 mM EDTA (buffer A) or capsid in 50 mM Sodium acetate, pH 5.0, 250 mM NaCl, 5 mM EDTA (buffer B) by velocity sedimenta-

tion through a 10–40% sucrose gradient (wt/vol) in the appropriate buffer. Sharp bands for capsid or procapsid were extracted directly from the tube with a syringe after centrifugation at 140,000 × *g*, 2 h in a Beckman SW28 rotor. Purified VLPs had a 260:280 ratio of 1.15–1.2. Alternatively, particles were treated with RNase prior to pelleting in sucrose to degrade ribosomal material (instead of EDTA). RNase treatment did not alter the 260:280 ratio of the final product, indicating that the packaged RNA was protected from degradation.

Protease digestions

NωV and HaSV samples at 10 mg/ml (10 μl) were digested with trypsin (Promega, Madison, WI) or Glu-C (Sigma) in either the procapsid or capsid form. The high pH procapsid buffer was 50 mM Tris–HCl, 250 mM NaCl, pH 7.6. The low pH maturation buffer was 50 mM Sodium acetate, 250 mM NaCl, pH 5.0. An enzyme to virus ratio of 1:1000 (wt/wt) was used in all reactions. Samples were diluted 10-fold with 10 mM acetic acid to arrest proteolysis at the specified time intervals and used directly for MALDI or SDS–PAGE analysis. The comparison between wild type and cleavage defective capsids was carried out using Glu-C in 50 mM phosphate, 250 mM NaCl at pH 5.0 and 7.6.

MALDI-TOF

Mass analysis was conducted on a Perceptive Biosystems Voyager Elite DE-STR. All spectra were acquired in reflectron mode with an accelerating voltage of 20,000, grid voltage 72%, and guide wire voltage 0.03%. Peptides were co-crystallized in either a saturated solution of 1,5-dimethoxy-4-hydroxycinnamic acid or 1-cyano-4-hydroxy-cinnamic acid in water/acetonitrile/TFA (50:50:0.05). Each sample was initially analyzed in both matrices, but the reported data are from α-cyano which had greater signal intensity and peptide coverage. Quantitation of released peptides was based on the ion intensity of peptides in a digest sample compared with the response of an internal ionization control. The protease digests were repeated 3 times, and each sample was analyzed in triplicate. 250 laser shots were averaged for each sample. Reported values are ion intensity of tryptic peptides/internal standard ion intensity.

Chemical labeling

VLPs at 1 mg/ml in buffer A were reacted with butanoic anhydride or acetic anhydride (1% vol/vol) for 2 h at room temperature. Biotin succinimidyl ester was dissolved in DMSO at 20 mg/ml and added to a final concentration of 2 mg/ml. Reactions were carried out at 4 °C for 16 h. After incubation, unreacted reagent was removed by extensive dialysis with a 10-kDa MWCO membrane or by exchanging the buffer with Biogel 30 spin columns (BioRad).

FT-IR

Fourier transform infrared spectroscopy was performed using a Bruker Tensor 37 model equipped with a biosampling cell (BioATRCell[TM] II, Bruker Optics Inc., Billerica). VLPs were at 7 mg/ml in buffer A made with D_2O. Exchange of protons for dueterons in the virus particles was accomplished by extensive dialysis, 48 h at 4 °C. 128 scans (in 100 s) were acquired for each measurement resulting in an average signal to noise ration of ~16,000 to 1. A matched D_2O buffer sample under identical conditions was used to subtract background. In the thermal denaturation experiments, 5 °C steps from 20 to 90 were used. The temperature was allowed to equilibrate for 10 min before each measurement. 128 scans were averaged at each temperature and the buffer/water vapor background was subtracted separately for each temperature.

Acknowledgments

References

Agrawal, D.K., Johnson, J.E., 1995. Assembly of the T = 4 Nudaurelia capensis omega virus capsid protein, post-translational cleavage, and specific encapsidation of its mRNA in a baculovirus expression system. Virology 207, 89–97.

Bothner, B., Dong, X.F., Bibbs, L., Johnson, J.E., Siuzdak, G., 1998. Evidence of viral capsid dynamics using limited proteolysis and mass spectrometry. J. Biol. Chem. 273 (2), 673–676.

Bothner, B., Schneemann, A., Marshall, D., Reddy, V., Johnson, J.E., Siuzdak, G., 1999. Crystallographically identical virus capsids display different properties in solution. Nat. Struct. Biol. 2, 114–116.

Brandon, C., Tooze, J., 1998. Introduction to Protein Structure, 2nd ed. Garland Publishing, New York, NY, pp. 300–304.

Canady, M.A., Tihova, M., Hanzlik, T.N., Johnson, J.E., Yeager, M., 2000. Large conformational changes in the maturation of a simple RNA virus, Nudaurelia capensis ω (NωV). J. Mol. Biol. 299, 573–584.

Canady, M.A., Tsuruta, H., Johnson, J.E., 2001. Analysis of rapid, large-scale protein quaternary structural changes: time-resolved X-ray solution scattering of Nudaurelia capensis ω (NωV) maturation. J. Mol. Biol. 311, 803–814.

Casal, H.L., Kohler, U., Mantsch, H.H., 1988. Structural and conformational changes of beta-lactoglobulin B: an infrared spectroscopic study of the effect of pH and temperature. Biochim. Biophys. Acta 957, 11–20.

Casper, D.L.D., Klug, A., 1962. Physical principles in the construction of regular viruses. Cold Spring Harbor Symp. Quant. Biol. 27, 1–24.

Cheng, R.H., Reddy, V.S., Olsen, N.H., Fisher, A.J., Baker, T.S., Johnson, J.E., 1994. Functional implications of quasi-equivalence in a T = 3 icosahedral animal virus established by cryo-electron microscopy and X-ray crystallography. Structure 2, 271–282.

Cohen, S.L., Ferre-D'Amare, A.R., Burely, S.K., Chait, B.T., 1995. Probing the solution structure of the DNA-binding protein Max by a combination of proteolysis and mass spectrometry. Protein Sci. 6, 1088–1099.

Conway, J.F., Wikoff, W.R., Cheng, N., Duda, R.L., Hendrix, R.W., Johnson, J.E., Steven, A.C., 2001. Virus maturation involving large subunit rotations and local refolding. Science 292, 744–748.

De Sena, J., Mandel, B., 1977. Studies on the in vitro uncoating of poliovirus: II. Characteristics of the membrane-modified particle. Virology 78, 554–566.

Fontana, A., Fassina, G., Vita, C., Dalzoppo, D., Zamai, M., Zambonin, M., 1986. Correlation between sites of limited proteolysis and segmental mobility in thermolysin. Biochemistry 25, 1847–1851.

Fenwick, M.L., Cooper, P.D., 1962. Early interactions between poliovirus and ERK cells. Some observation on the nature and significance of the rejected particles. Virology 15, 212–223.

Fricks, C.E., Hogle, J.M., 1990. Cell-induced conformational change in poliovirus: externalization of the amino terminus of VP1 is responsible for liposome binding. J. Virol. 64, 1934–1945.

Helgstrand, C., Munshi, S., Johnson, J.E., Liljas, L., 2004. The refined structure of Nudaurelia capensis omega virus reveals control elements for a T = 4 capsid maturation. Virology 318, 192–203.

Hogle, J.H., 2002. Poliovirus cell entry: common structural themes in viral cell entry pathways. Annu. Rev. Microbiol. 56, 777–802.

Janshoff, A., Bong, D.T., Steinem, C., Johnson, J.E., Ghadiri, M.R., 1999. An animal virus-derived peptide switches membrane morphology: possible relevance to nodaviral transfection processes. Biochemistry 38, 5328–5336.

Johnson, J.E., 2003. Virus particle dynamics. Adv. Protein Chem. 64, 197–218.

Joklik, W.K., Darnell, J.E., 1961. The adsorption and early fate of purified poliovirus in HeLA cells. Virology 13, 439–447.

Krimm, S., Bandekar, J., 1986. Vibrational spectroscopy and conformation of peptides, polypeptides, and proteins. Adv. Protein Chem. 38, 181–364.

Kriwacki, R.W., Wu, J., Siuzdak, G., Wright, P.E., 1996. Probing protein/protein interactions with mass spectrometry and isotopic labeling: analysis of the p21/Cdk2 complex. J. Am. Chem. Soc. 118, 5320–5321.

Lee, K.K., Tang, J., Taylor, D., Bothner, B., Johnson, J.E., 2004. Small compounds targeted to subunit interfaces arrest maturation in a nonenveloped, icosahedral animal virus. J. Virol. 78, 7208–7216.

Lewis, J.K., Bothner, B., Smith, T.J., Siuzdak, G., 1998. Antiviral agent blocks breathing of the common cold virus. Proc. Natl. Acad. Sci. U.S.A. 95, 6774–6778.

Li, Q., Yafal, A.G., Lee, Y.M.-H., Hogle, J., Chow, M., 1994. Poliovirus neutralization by antibodies to internal epitopes of VP4 and VP1 results from reversible exposure of these sequences at physiological temperature. J. Virol. 68, 3965–3970.

Liu, H., Qu, C., Johnson, J.E., Case, D.A., 2003. Pseudo-atomic models of swollen CCMV from cryo-electron microscopy data. J. Struct. Biol. 142, 356–363.

Mosser, A.G., Shepard, D.A., Rueckert, R.R., 1994. Use of drug-resistance mutants to identify functional regions in picornavirus capsid proteins. Arch. Virol., Suppl. 9, 111–119.

Munshi, S., Lijas, L., Cavarelli, J., Bomu, W., McKinney, B., Reddy, V., Johnson, J.E., 1996. The 2.8 A structure of a T = 4 animal virus and its implications for membrane translocation of RNA. J. Mol. Biol. 261, 1–10.

Oliveira, A.C., Gomes, A.M., Almeida, F.C., Mohana-Borges, R., Valente, A.P., Reddy, V.S, Johnson, J.E., Silva, J.L., 2000. Virus maturation targets the protein capsid to concerted disassembly and unfolding. J. Biol. Chem. 275, 16037–16043.

Phelps, D.K., Post, C.B., 1995. A novel basis for capsid stabilization by antiviral compounds. J. Mol. Biol. 254, 544–551.

Prevelige, P.E., Thomas Jr., D., Aubrey, K.L., Towse, S.A., Thomas Jr., G.J., 1993. Subunit conformational changes accompanying bacteriophage P22 capsid maturation. Biochemistry 32, 537–543.

Prevelige Jr., P.E., 1998. Inhibiting virus-capsid assembly by altering the polymerisation pathway. Trends Biotechnol. 16, 61–65.

Reddy, V.S., Natarajan, P., Okerberg, B., Li, K., Damodaran, K.V., Morton, R.T., Brooks III, C.L., Johnson, J.E., 2001. Virus particle explorer (VIPER), a website for virus capsid structures and their computational analysis. J. Virol. 75, 11943–11947.

Reisdorph, N., Thomas, J.J., Katpally, U., Chase, E., Harris, K., Siuzdak, G., Smith, T.J., 2003. Human rhinovirus capsid dynamics is controlled by canyon flexibility. Virology 314, 34–44.

Schultz, C.P., 2000. Illuminating folding intermediates. Nat. Struct. Biol. 7, 7–10.

Taylor, D., Krishna, N.K., Candy, M.A., Scheenmann, A., Johnson, J.E., 2002. Large-scale, pH-dependent, quaternary structure changes in an RNA virus capsid are reversible in the absence of subunit autoproteolysis. J. Virol. 76, 9972–9980.

Taylor, D., Wang, Q., Bothner, B., Natarajan, P., Finn, M.G., Johnson, J.E., 2003. Correlation of chemical reactivity of Nudaurelia capensis omega virus with a pH-induced conformational change. Chem. Commun. (Cambridge) 22, 2770–2771.

Teschke, C.M., King, J., Prevelige Jr., P.E., 1993. Inhibition of viral capsid assembly by 1,1′-bi(4-anilinonaphthalene-5-sulfonic acid). Biochemistry 32, 10658–10665.

Vriend, G., Verduin, B.J., Hemminga, M.A., 1986. Role of the N-terminal part of the coat protein in the assembly of cowpea chlorotic mottle virus. A 500 MHz proton nuclear magnetic resonance study and structural calculations. J. Mol. Biol. 191, 453–460.

Witz, J., Brown, F., 2001. Structural dynamics, an intrinsic property of viral capsids. Arch. Virol. 146, 2263–2274.

Zlotnick, A.P., Ceres, P., Singh, S., Johnson, J.M., 2002. A small molecule inhibits and misdirects assembly of hepatitis B virus capsids. J. Virol. 76, 4848–4854.

Zurdo, J., Guijarro, J.I., Dobson, C.M., 2001. Preparation and characterization of purified amyloid fibrils. J. Am. Chem. Soc. 123, 8141–8142.